Biochemistry and Biophysics Reports 9 (2017) 100–105

Contents lists available at ScienceDirect

Biochemistry and Biophysics Reports

journal homepage: www.elsevier.com/locate/bbrep

Engineering microdent structures of bone implant surfaces to enhance osteogenic activity in MSCs

Sophia Li, Thomas Chow, Julia Chu*

Department of Bioengineering and The Center for Tissue Engineering, University of California, Berkeley, CA, USA

ARTICLE INFO

Keywords:
Micropatterns
Bone implants
Microdents
Mesenchymal stem cells
Osteogenic differentiation

ABSTRACT

Problems persist with the integration of hip and dental implants with host bone tissues, which may result in long-term implant failure. Previous studies have found that implants bearing irregular surfaces can facilitate osseointegration. An improvement to this approach would use implant surfaces harboring a well-defined surface microstructure to decrease variability in implant surfaces. In this study, we tested whether well-defined surfaces with arrays of microdents (each with depth approximately 3 μm) significantly affected the morphology, proliferation, and osteogenic activity of mesenchymal stem cells (MSCs). Arrays of microdents tested had diameters of 9 μm, 12 μm, and 18 μm, while spacing between arrays ranged from 8 μm to 34 μm. Effects on MSC morphology (cell spreading area) and proliferation were also quantified, with both significantly decreasing on micropatterned surfaces ($p < 0.05$) on smaller and denser microdents. In contrast, MSCs were found to deposit more calcified matrix on smaller and denser arrays of microdents. MSCs on a pattern with arrays of microdents with a diameter of 9 μm and a spacing 8 μm deposited 3–4 times more calcified matrix than on a smooth surface ($p < 0.05$). These findings show that well-defined surface microtopographies promote osteogenic activity, which can be used on implant surfaces to improve integration with the host bone tissue.

1. Introduction

Bone and dental implants are frequently used to repair fractured or injured bone, joints and teeth. For example, osteoarthritis of the hip alone results in over 200,000 hip replacements annually. Failure of the prosthesis is a dangerous, burdensome, and costly complication, resulting in 37,000 revision hip replacements annually in the US, procedures which cost the nation over one billion dollars annually [1]. Given these numbers, the failure rate impacts a huge number of people and adds considerable cost to the healthcare system [2]. The most common reason for these failures is the loosening and detachment of the implant from the bone due to wear, or from poor integration with the bone. In the United States, around 600,000 cases of poor union and 100,000 cases of complete nonunion of implants with the surrounding tissue are reported every year [3]. An important challenge is the development of biomimetic matrices with particular geometry and porosity that direct cell differentiation to bone formation.

Soon after implantation, MSCs in the bone marrow and surrounding tissues migrate to the bone-implant interface and participate in the matrix remodeling. MSCs are capable of differentiating into osteoblasts and have been used in vitro to study cell-material interactions and osteoblastogenesis [4,5]. Because there are many biophysical and biochemical factors that influence cellular differentiation, there have been many attempts to control or impose these factors to promote osteogenic differentiation, such as surface topography [6]. Some studies have shown that repetitive concavitives of highly crystalline or biphasic hydroxyapatite/ b-tricalcium phosphate promote osteoconduction and osteoinduction in primates [7,8]. Other studies have shown that implants whose interfacial surfaces are roughened by sandblasting can exhibit improved integration with host bone compared to implants with smooth surfaces [9]. The mechanism underlying this improvement is not fully understood, in part because this surface roughening procedure cannot be controlled, which may lead to sample-to-sample variability. This limitation is addressed in this study through the development of implants whose surfaces are engineered with defined microtopography that allow us to quantitatively evaluate the effect of surface microstructure on the growth and differentiation of MSCs and the deposition of calcified matrix at the bone-implant interface.

Micropatterns have been shown to regulate many aspects of cell function and behavior, including their morphology, migration, proliferation, and differentiation. For example, a recent study found that square-patterned coatings of diamond, titanium, tantalum and chromium result in reduced cell-spreading compared to cell-spreading

* Corresponding author.
E-mail address: Juliachu@berkeley.edu (J. Chu).

http://dx.doi.org/10.1016/j.bbrep.2016.11.016
Received 22 July 2016; Received in revised form 28 November 2016; Accepted 30 November 2016
Available online 10 December 2016

areas recorded on the same material with a smooth surface [10]. Moreover, the authors proposed that cells attached to surfaces with square-shaped microstructures produced bone less effectively than cells on a smooth surface. Another study showed that cell adhesion and the proliferation of mesenchymal stem cells (MSCs) seeded on island-patterned (randomly-sized round posts) poly(lactic acid) membranes (60–100 μm) were higher compared to cells grown on membranes with a smooth surface [11]. In the same study, MSCs were also shown to maintain their potential to differentiate into bone cells. However, it is not apparent from a review of literature what types and sizes of surface microtopography is best suited to promote the production of bone matrix. Other studies have shown that micropost or microgroove-based microtopographic surfaces may regulate cell functions such as morphology and proliferation and may promote differentiation [12]. To transfer these well-defined micropatterns, prevalent methods such as laser-sintering may be used [13,14].

We hypothesized that surfaces composed of defined arrays of microdents would promote osteogenic differentiation and the regulation of calcified matrix deposition by bone cells compared to that on a smooth surface. To test our hypothesis, we designed surfaces with various arrays of microdents in well-defined size and spacing, and determined their effects on cell morphology, proliferation, and the deposition of calcified matrices.

2. Materials and methods

2.1. Human MSC culture

Human MSCs were obtained commercially from Lonza Corp. MSC cultures were maintained with MSC basal medium with MSC growth supplement, L-glutamine, and GA-1000 in an incubator at 37 °C. Cells were maintained in a humidified 95% air–5% CO_2 incubator at 37 °C. All experiments used cultures prior to passage 10.

2.2. Cell passaging

MSCs were maintained in 100 mm culture dishes and passaged every two days to prevent confluence and differentiation. After the media was removed, cells were washed with phosphate buffer saline (PBS), and then detached following incubation with 3 mL 0.5x trypsin for 4 min. MSC media (7 mL) was then added to the dish to neutralize the trypsin. The cells in suspension were collected and centrifuged at 1000 rpm for 4 min. The supernatant was removed and the cells were resuspended in 10 mL MSC media and seeded in new 100 mm tissue culture dishes.

2.3. Microfabrication to make micropatterned membranes

Polydimethylsiloxane (PDMS) membranes with micro-patterned dents were fabricated to test the effects of specific surface microtopographies on MSC differentiation and subsequent deposition of calcified matrix. First, a thickness of 3-μm SU-8 negative epoxy photoresist was spin coated and soft baked to attach on a silicon wafer. A high resolution photomask with arrays of different diameter and spacing circles was aligned with the photoresist coated wafer. UV light was directed through the photomask, which resulted in crosslinking only UV-exposed regions of the photoresist. A post exposure bake is performed to complete the polymerization. Then, the wafer is immersed in SU-8 developer to wash away the non-cross linked photoresist. Finally, the wafer is rinsed with isopropanol, dried with nitrogen gas, and hard baked to cure the material. The wafer, imprinted with the micropatterned photoresist, was used as a mold to cast the same micropattern onto PDMS membranes. In particular, a PDMS elastive base was mixed thoroughly with elastive curing agent in a 10:1 ratio and placed in the vacuum to remove air bubbles. The mixture was then poured onto the silicon wafer bearing a specific micropattern, including those with a smooth surface, which served as a control. The silicon wafer was evenly coated with the PDMS mixture after being spun in the Horace machine at 220 rpm for 120 s. The wafer was baked at 80 °C for 45 min, and the elastic PDMS membrane carefully peeled off the wafer using tweezers. The micropatterned membranes were further processed for cell seeding experiments.

2.4. Cell seeding

The PDMS membranes were cleaned in 70% ethanol for 15 min using a bath sonicator. After being air-dried, the membranes were exposed to an oxygen plasma for 1 min. The PDMS surface was then coated with a gelatin suspension for 30-min while being exposed to a UV-light source. Following rinses with ethanol and PBS, the membranes were placed in 100 mm culture dishes and used as a substrate to support cell growth.

2.5. Fluorescence staining of actin filaments and microscopy

Cells attached to gelatin-coated PDMS membranes were maintained for 2 days in the incubator prior to staining. They were then washed with PBS and fixed with 4% paraformaldehyde for 15 min, and permeabilized with 0.5% Triton X-100 for 10 min. These fixed cell preparations were stained for actin filaments using a 1:100 dilution of 6.6 μM Alexa Fluor 546 phalloidin, and incubated in the dark at room temperature for 45 min. The nuclei of the fixed cells were then stained with 1:1000 dilution of 300 μM DAPI. After washings with PBS, fixed cell preparations were mounted on a glass slide and preserved using the Vectashield mounting medium. These samples were imaged with a Zeiss Axio Imager 2 fluorescent microscope and analyzed with ImageJ software to quantify the spreading area of cells.

2.6. Cell proliferation assay

Cells were fixed and stained to measure proliferation after 1 d of being maintained in an incubator. The rate of cell proliferation was measured using a 5-Ethyl-2′-deoxyuridine (EdU) proliferation assay purchased from Invitrogen, Corp. (San Diego, CA). Proliferating cells incorporate EdU into newly synthesized DNA, which was detected and quantified by imaging the fluorescence of a click-chemistry based stain for EdU in the nucleus. Briefly, EdU was added to the culture media and after a 2-h incubation, the media was removed and the cells were fixed with 4% paraformaldehyde for 15 min, and washed twice in 3% bovine serum albumin (BSA) in PBS. These cells were permeabilized with 0.5% Triton X-100 for 20 min. The cells were incubated with the EdU-binding Alexa Fluor 488 azide probe for 20 min in the dark, and the nucleus was counter-stained using a 1:1000 dilution of 300uM DAPI. These stained cell preparations were mounted on slides and imaged using a Zeiss Axio Imager 2 fluorescence microscope. Images of EdU and DAPI staining were recorded in the FITC and DAPI channels and analyzed with ImageJ software to quantify the number of proliferating cells (those that stained positive for EdU) and the total number of cells sampled in these studies. Cell proliferation rate was calculated as the percentage of cells in the sample that incorporated EdU after 2 h of incubation, though all samples were compared relatively to cell proliferation on the control surface.

2.7. Osteogenic differentiation of mscs and the deposition of calcified matrix

MSC were cultured on micropatterned or control surfaces in osteogenic media for 2 weeks in order to induce osteogenic differentiation and deposition of a calcified matrix. The differentiating osteogenic media was composed of DMEM supplemented with 10% fetal bovine serum, 1% penicillin/streptomycin, 200 uM ascorbic acid, and 0.1 uM dexamethasone, and 10 mM b-glycerophosphate. Since MSCs do not

deposit a calcified matrix on gelatin substrates, then the deposition of a calcified matrix on test and control membranes plated with MSCs must arise from their differentiation to osteoblasts. Osteogenic differentiation of MSCs on the micropatterned surfaces was determined using the Alizarin Red staining assay. Alizarin Red complexes with calcium and produces a red stain that can be quantified from images recorded using bright-field light microscopy. The Alizarin Red solution was prepared by mixing 1 g of Alizarin Red S in 50 mL distilled water (adjust solution pH to 4.3). Micropatterned and control samples were first washed with PBS and then incubated with the diluted Alizarin Red solution for 5 min. The cells were subsequently washed with distilled water and mounted on glass slides for transmitted light imaging using the Zeiss Axio Imager 2 microscope. The images were processed and analyzed with ImageJ software in order to find the percentage area of red, positively stained calcified matrix over total surface area.

2.8. Statistical analysis

StatPlus software was used to run statistical analysis in Microsoft Excel. All data are presented in graphs as +/- standard error. One-way analysis of variance (ANOVA) was used to calculate significance between each data set group; $p < 0.05$ was considered significant.

3. Results

3.1. Fabrication of micropatterns on PDMS membrane

We designed micropatterns with surface microdents having three distinct diameters: 9 μm (A1-A4), 12 μm (B1-B4) and 18 μm (C1-C4). Each pattern was composed of arrays of microdents with different spacing (Table 1). Measurements of the diameter of the microdent in each pattern and the distance between a horizontal pair of microdents within the array are presented in Table 1 (A1~A4, B1~B4 and C1~C4). (Fig. 1).

3.2. Effects of micropatterned surfaces on cell morphology

Morphology of MSCs attached to each of the micropatterned surfaces was analyzed by quantifying cell-spreading area (Fig. 2). MSCs on the control surface (smooth surface without a micropattern) were well-spread with an average area of 9700 μm^2, and used as a reference for cells cultured on other substrates. MSCs attached to all micropatterned surfaces exhibited significantly lower cell-spreading than MSCs on the control surface ($p < 0.05$, n=6). The only statistically significant difference found between micropatterns was between patterns A4 and B1. A table with p-values between significantly different patterns is provided in Supplementary Data.

MSCs seeded on patterns A1-A4, with the smallest diameter microdents (9 μm) had areas ranging from 4700 μm^2 to 5600 μm^2. MSCs attached to surfaces B1-B4 and C1-C4 (larger microdent diameters 12 μm and 18 μm, respectively) had cell areas ranging from 5700 μm^2 to 7700 μm^2.

Table 1
Dimensions of Micropatterned Surfaces. For a given microstructured pattern, the letters A, B and C reflect the progression of diameter size (9,12 and 18 μm respectively), whereas larger distances between microdents are indicated by a higher number (1–4).

Pattern	Dent diameter (μm)	Spacing (μm)
A1	9	8
A2	9	10
A3	9	12
A4	9	18
B1	12	8
B2	12	12
B3	12	18
B4	12	22
C1	18	12
C2	18	20
C3	18	28
C4	18	34

3.3. Effects of micropatterned surfaces on cell proliferation

As shown in Fig. 3, the rate of cell proliferation was generally significantly lower on micropatterned surfaces compared to the control (flat) surface (n=4), with the exceptions of patterns C3 (18 μm dent diameter and 28 μm spacing) and C4 (18 μm and 34 μm spacing), which have the largest microdent size and spacings. A statistically significant difference in proliferation on micropatterned surface occurred between patterns A4 and B1, B1 and B3, B2 and B3, and A4 and C1. A table with p-values between significantly different patterns is provided in Supplementary Data.

3.4. Effects of micropatterned surfaces on matrix calcification

MSCs on arrays of microdents were found to deposit higher levels of calcified matrix compared to MSCs on the control surface (Fig. 4). In order to statistically compare the amounts of matrix mineralization on each surface, we used ImageJ software to quantify the percent of positively stained red calcified matrix over the total surface area (n=4). On average, the area of calcified matrix on the control surface was 10.5% of the total area in a given image. Surfaces with smaller microdent size and spacing (A1-A4 and B1-B2) have significantly more ($p < 0.05$) calficied matrix than the control surface, whereas surfaces with large microdent size and spacing (B3-B4, C1-C4) did not show significant differences in calcified matrix from the control. The data also indicated that cells deposited the highest amounts of calcified matrix on surfaces with the smallest, most densely packed microdents. On surface A1, calcified matrix was 38% of the given area, almost 4 times as much as on the control surface.

There were some statistically significant ($p < 0.05$) differences between the following pairs of micropatterned surfaces: A1 and all other patterns, A2 and C3, A2 and C4, A3 and B3, A3 and B4, A3 and C2, A3 and C3, A3 and C4, A4 and B3, A4 and B4, A4 and C2, A4 and C3, A4 and C4, B1 and B3, B1 and C2, B1 and C3, B1 and C4, B2 and B3, B2 and C2, B2 and C3, B2 and C4, B4 and C2, B4 and C3, C1 and B3, C3 and C4. A table with p-values between significantly different patterns is provided in Supplementary Data.

In summary, MSCs produced more calcified matrix on patterns with relatively smaller dents and smaller spacing between arrays of microdents. MSCs on patterns with a large spacing (> 18 μm) and larger dent diameter (18 μm) produced similar amounts of calcified matrix to MSCs on the control surface. Thus, an increase in spacing between microdents correlated with a decrease in matrix deposition. This finding was most obvious for cells attached to surfaces in group A, most likely because the increase in microdent spacing is larger relative to the diameter of their microdents.

4. Discussion

In summary, results presented in this study have shown that that MSC differentiation to bone cells, and the deposition of calcification matrix is improved on substrates that harbor a defined structure of microdents compared to that on smooth surfaces. The deposition of calcified matrix is dependent on both the diameter of the microdents and the spacing between arrays of microdents. Microstructured pattern A1 produced the most calcified matrix (37.7% calcified matrix percent area compared to control surface 10.5%); this pattern had the smallest dent size and smallest spacing between microdents in the sampled micropatterns. For microdent arrays that are too sparse or have diameters too large, MSC matrix calcification on micropatterned surfaces is similar as on the control surface. For example, cells attached

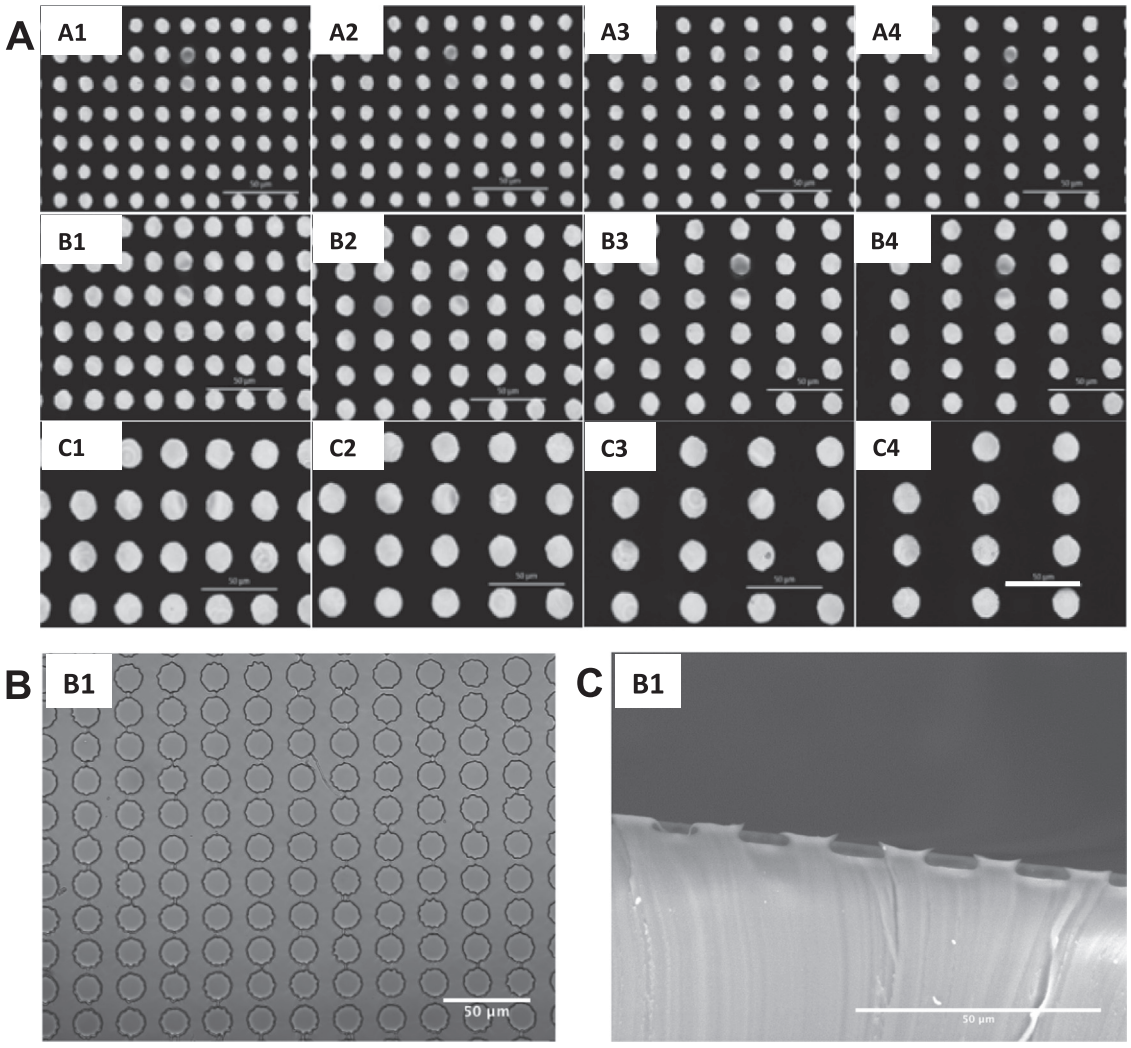

Fig. 1. Images of micropatterns. (A) Images of the photomasks used to make microtopographic features on silicon wafer. Scalebar=50 µm. These patterns and their names are referenced throughout the following figures. (B) Image of pattern B1 microtopographic surface fabricated with PDMS using confocal microscope. Scalebar=50 µm. (C) Membrane was cut to show the sideview of microdents. Sideview of pattern B1 microdents using Scanning Electron Microscopy (SEM) is shown. Scalebar=50 µm.

to substrates with a sparse array of microdents were found to produce less calcified matrix compared to those attached to dense arrays of microdents. Similarly, cells attached to surfaces with large diameter microdents did not produce as much calcified matrix as those attached to smaller microdents. The microdent size was found to be the major determining factor in producing calcified matrix rather than the spacing between microdent arrays; as microdent diameter increased from 9 µm in group A to 18 µm, there was a steady decrease in matrix calcification and significant differences from the control. It must be said however, that these decreases in matrix calcification are magnified

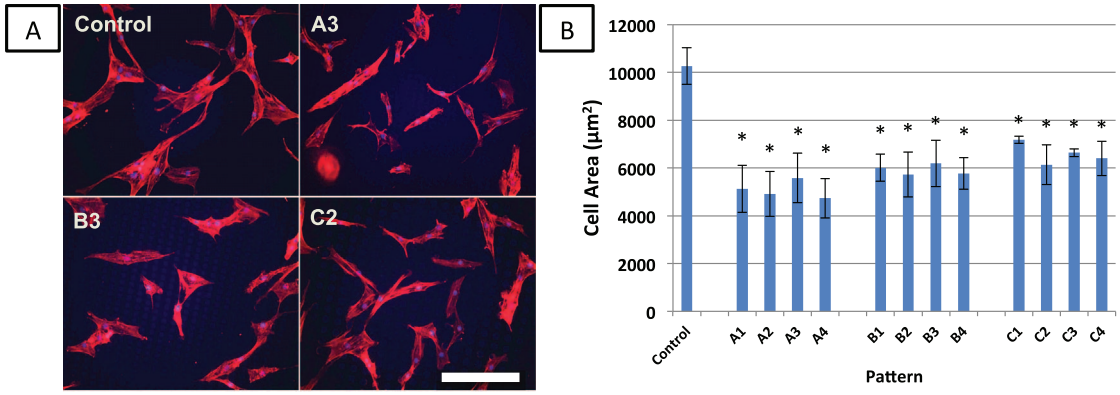

Fig. 2. Effect of microtopography on cell spreading and morphology. (A) hMSCs were cultured on microtopographic surfaces for one day and then fixed and stained for fluorescent microscopy of actin filaments (red). Fluorescent microscopy was used image samples. Scale bar=250 µm. Control is a smooth, flat surface. (B) cell areas on microdent surfaces were quantified with ImageJ. Brightness and contrast were increased for greater ease of image analysis. Error bars represent mean ± standard error (n=6). *significantly different from control, $p < 0.05$. A table with p-values between significantly different patterns is provided in Supplementary Data.

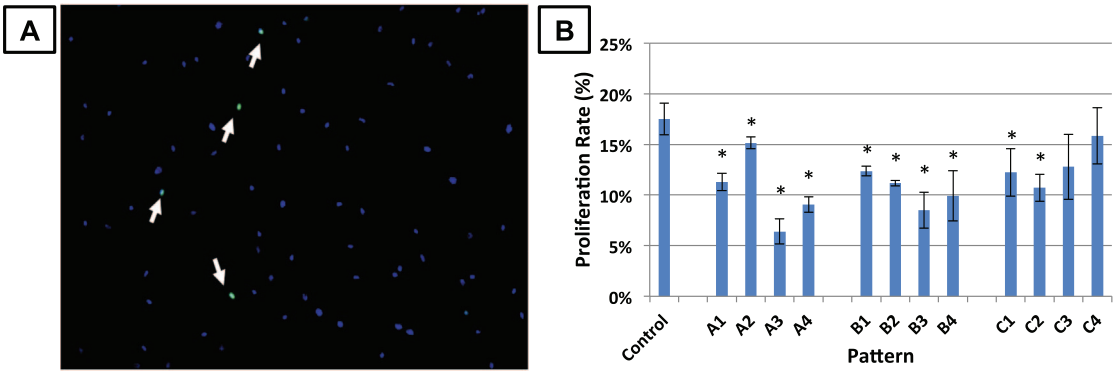

Fig. 3. Effect of microtopography on cell proliferation. MSCs were cultured on microtopographic surfaces for one day and proliferative cells were labeled with EdU during 2 h of incubation. (A) The cells were then fixed and stained for EdU (green, indicated with arrows) and nucleus (blue). (B) The percentage of EdU-positive cells were counted and divided by the proliferation rate on control (flat) surfaces. Error bars represent mean ± standard error (n=4). *significantly different from control, $p < 0.05$. A table with p-values between significantly different patterns is provided in Supplementary Data.

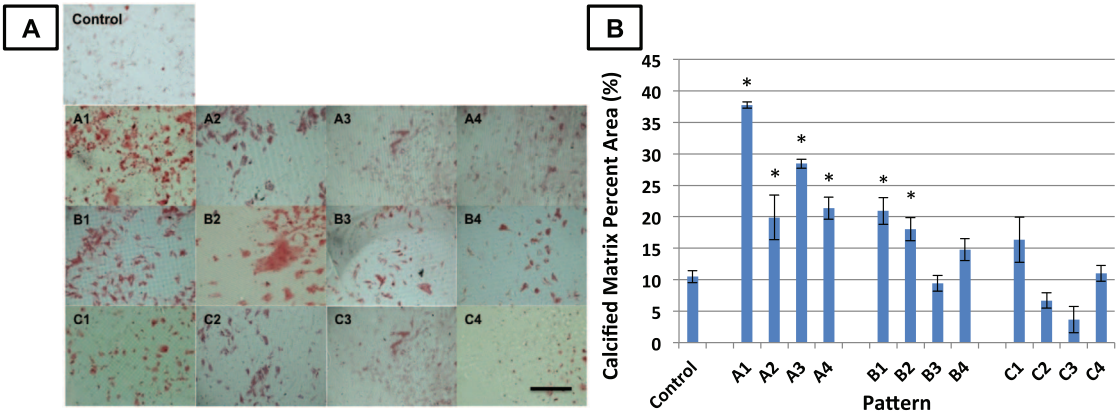

Fig. 4. Effect of microtopography on matrix calcification. (A) The cells were cultured on microtopographic surfaces for 3 weeks in osteoblastogenic medium. They were then fixed and stained for deposition calcified matrix with Alizarin Red (red). Scalebar=1 mm. (B) Percent area of positively stained calcified matrix was quantified with ImageJ. Error bars represent mean ± standard error (n=4). *significantly different from control, $p < 0.05$. A table with p-values between significantly different patterns is provided in Supplementary Data.

within groups as spacing increases – in this context, microdent array spacing may still be considered a factor in the optimization of matrix calcification by attached MSCs.

An interesting note is that the rate of cell proliferation and cell spreading area are lower on the micropatterned surfaces. The exception is that proliferation patterns C3 and C4 with largest microdent size and spacings did not show differences from the control.

The driving force for the work presented in this study was to improve the efficiency of the integration of artificial implants onto bone. Previous studies have shown that implants that have implants that have sandblasted and island structured (i.e. randomized micropost arrays) surfaces are more efficiently integrated in bone compared to those with smooth surfaces [4,6]. Our findings on the effects of microdents can help to further improve bone production on bone-implant interfaces under a well-defined and controlled condition.

This study investigated the effects of surface topography on MSC functions on the microscale; however, there has also been research into the use of surface topography at the nanoscale on biomaterials. Studies have shown that nanotopography can also promote osteogenic differentiation and other functions such as proliferation in vitro, even in the absence of osteoinductive media [15] or other signals [16]. Whether microtopography or nanotopography is used to regulate MSC osteogenic differentiation and activity, both indicate that the use of surface topography can be an important biophysical factor in directing MSC activity.

The micropatterned surface that were identified in this study as promoting bone integration can be easily reproduced on the surfaces of titanium based bone and dental implants. Methods to transfer specific micropatterns to titanium surfaces for bone implant surfaces include laser sintering and mask-directed chemical modification, acid-etching and anodization, with laser sintering being the most common [17,18]. In recent years, titanium materials fabricated by direct laser metal sintering (DLMS) have been used for dental implants with good controlled porosity, surface microstructure closer to bone which are capable to build 3D model from titanium or its alloy powders [13]. This method of laser sintering offers an easy method of translation for micropatterned surfaces on materials used in prosthesis for hip replacement and dental replacements [14]. However, there are a few limitations that may addressed in future research. For example, the potential beneficial effects of the investigated micropatterned surfaces have not been attempted in studies in vivo. In addition, based on trends that indicated that smaller and denser microdent arrays are ideal for matrix calcification, a larger range of micropatterned arrays may be explored.

In summary, our findings have identified novel surface microtopographies designs for bone and dental prostheses that promote bone matrix production at the bone-implant interface. Our findings identify a new approach for the design of bone implants that is expected to improve the integration of implanted structures into host materials. This may thereby improve outcomes of clinical therapies for hundreds of thousands of patients a year who report problems with their implants with concomitant savings in the cost of follow-up and corrective healthcare.

Acknowledgments

We thank Professors Gerard Marriott and Song Li for their guidance and support. All experiments were performed in the Department of Bioengineering at UC Berkeley.

Appendix A. Transparency document

Transparency data associated with this article can be found in the online version at http://dx.doi.org/10.1016/j.bbrep.2016.11.016.

Appendix B. Supporting material

Supplementary data associated with this article can be found in the online version at http://dx.doi.org/10.1016/j.bbrep.2016.11.016.

References

[1] J.N.Katz, J.Wright, E.A.Wright, E.Losina, Failures of total hip replacement: a population-based perspective, Orthop. J. Harvard Med. Sch., vol. 9, pp. 101–106.
[2] Ted Xenodemetropoulos, Shawn Davison, George Ioannidis, Jonathan D. Adachi, The impact of fragility fracture on health-related quality of life, Drugs Aging 21.11 (2004) 711–730 (Web).
[3] J.A. Bishop, A.A. Palanca, M.J. Bellino, D.W. Lowenberg, Assessment of compromised fracture healing, J. Am. Acad. Orthop. Surg. 20 (5) (2012) 273–282.
[4] B.érengère J.C. Luthringer, M.R. Katha Uma, Regine Willumeit, Phosphatidylethanolamine biomimetic coating increases mesenchymal stem cell osteoblastogenesis, J. Mater. Sci.: Mater. Med. 25.11 (2014) 2561–2571 (Web. 11 Oct. 2016).
[5] B.érengère Jc Luthringer, Regine Willumeit-Römer, Effects of magnesium degradation products on mesenchymal stem cell fate and osteoblastogenesis, Gene 575.1 (2016) 9–20 (Web. 11 Oct. 2016).
[6] Giulio Abagnale, Michael Steger, Vu. Hoa Nguyen, Nils Hersch, Antonio Sechi, Sylvia Joussen, Bernd Denecke, Rudolf Merkel, Bernd Hoffmann, Alice Dreser, Uwe Schnakenberg, Arnold Gillner, Wolfgang Wagner, Surface topography enhances differentiation of mesenchymal stem cells towards osteogenic and adipogenic lineages, Biomaterials 61 (2015) 316–326 (Web. 21 Oct. 2016).
[7] U. Ripamonti, E. Tsiridis, C. Ferretti, C.J. Kerawala, A. Mantalaris, M. Heliotis, Perspectives in regenerative medicine and tissue engineering of bone, Br. J. Oral. Maxillofac. Surg. 49 (7) (2011) 507–509.
[8] M. Heliotis, U. Ripamonti, C. Ferretti, C. Kerawala, A. Mantalaris, E. Tsiridis, The basic science of bone induction, Br. J. Oral. Maxillofac. Surg. 47 (7) (2009) 511–514.
[9] D. Buser, R.K. Schenk, S. Steinemann, J.P. Fiorellini, C.H. Fox, H. Stich, Influence of surface characteristics on bone integration of titanium implants. A histomorphometric study in miniature pigs, J. Biomed. Mater. Res. 25 (1991) 889–902.
[10] S. Myllymaa, E. Kaivosoja, K. Myllymaa, T. Sillat, H. Korhonen, R. Lappalainen, et al., Adhesion, spreading and osteogenic differentiation of mesenchymal stem cells cultured on micropatterned amorphous diamond, titanium, tantalum and chromium coatings on silicon, J. Mater. Sci. Mater. Med 21 (2010) 329–341.
[11] I.C. Lee, Y.T. Lee, B.Y. Yu, J.Y. Lai, T.H. Young, The behavior of mesenchymal stem cells on micropatterned PLLA membranes, J. Biomed. Mater. Res. A 91A (2009) 929–938.
[12] J. Li, M. Wu, J. Chu, R. Sochol, S. Patel, Engineering micropatterned surfaces to modulate the function of vascular stem cells, Biochem. Biophys. Res. Commun. 444 (2014) 562–567.
[13] T. Traini, C. Mangano, R.L. Sammons, F. Mangano, A. Macchi, A. Piattelli, Direct laser metal sintering as a new approach to fabrication of an isoelastic functionally graded material for manufacture of porous titanium dental implants, Dent. Mater. 24 (11) (2008) 1525–1533.
[14] Jamil A. Shibli, Carlo Mangano, Francesco Mangano, José A. Rodrigues, Alessandra Cassoni, Karen Bechara, Jose Divino B. Ferreia, Alexandre M. Dottore, Giovanna Iezzi, Adriano Piattelli, Bone-to-implant contact Around immediately loaded Direct laser metal-forming transitional implants in human posterior maxilla, J. Periodontol. 84.4 (2013) 732–737 (Web. 11 Oct. 2016).
[15] Sander Dobbenga, E. Fratila-Apachitei Lidy, Amir A. Zadpoor, Nanopattern-induced osteogenic differentiation of stem cells – A systematic review, Acta Biomater. (2016) (n. pag. Web. 21 Oct. 2016).
[16] Mun-Jung Kim, Bora Lee, Kisuk Yang, Junyong Park, Seokwoo Jeon, Soong Ho Um, Dong-Ik Kim, Sung Gap Im, Seung-Woo Cho, "MP-2 peptide-functionalized Nanopatterned substrates for enhanced osteogenic differentiation of human mesenchymal stem cells, Biomaterials 34.30 (2013) 7236–7246 (Web. 21 Oct. 2016).
[17] Zu-yong Wang, et al., Enhancing mesenchymal stem cell response using uniaxially stretched poly (ε-caprolactone) film micropatterns for vascular tissue engineering application, J. Mater. Chem. B 2.35 (2014) 5898–5909.
[18] Chunyong Liang, Hongshui Wang, Jianjun Yang, Yanli Cai, Xin Hu, Yang Yang, Baoe Li, Hongjie Li, Haipeng Li, Changyi Li, Xianjin Yang, Femtosecond laser-induced micropattern and Ca/P deposition on Ti implant surface and its acceleration on early osseointegration, ACS Appl. Mater. Interfaces ACS Appl. Mater. Interfaces 5.16 (2013) 8179–8186 (Web. 21 Oct. 2016).